WWU Honors College Senior Projects   WWU Graduate and Undergraduate Scholarship

Spring 2023

Synthesis and characterization of hydroxy-functionalized copper indium disulfide quantum dots

Julia Schexnayder

Synthesis and characterization of hydroxy-functionalized copper indium disulfide quantum dots

Julia Schexnayder*, Dr. David A. Rider

Undergraduate Honors Thesis in Fulfillment of CHEM 498, Spring 2023

Department of Chemistry, Western Washington University, 516 High Street, Bellingham, WA 98225-9150

schexnj@wwu.edu

ABSTRACT: Quantum dots offer tunable electronic and optical properties due to the quantum confinement effect, making them desirable for various applications. However, their native hydrophobic form requires surface chemistry modification for certain applications. This research explores the method of ligand exchange using 11-mercapto-1-undecanol for improving the stability of copper indium disulfide (CIS) quantum dot (QD) nanoparticles in polar environments. The effects of this ligand exchange on QD chemical composition, optical properties, hydroxy-reactivity, and hydrodynamic radius are characterized. Analysis of characterization results indicates successful surface modification through hydroxy-functionalization, as confirmed by ^{1}H-NMR and IR spectroscopy. The desired optical properties of the QDs are retained post-surface modification, with no significant reduction in quantum yield. Additionally, the reaction of hydroxy-functionalized QDs with toluene diisocyanate (TDI) demonstrates successful binding of the hydroxy groups, indicating the suitability of ligand-exchanged QDs for further reactions and processing needed for future applications. Particle size comparison via differential light scattering reveals that ligand-exchanged QDs maintain a relatively small size compared to other hydroxy-functionalization methods. Overall, the ligand exchange method shows promise for enhancing the stability and biocompatibility of QDs, unlocking potential applications in nanotechnology previously not accessible.

INTRODUCTION

In the realm of materials science and nanotechnology, quantum dot (QD) semiconductor nanoparticles pose an exciting research frontier. When compared to more traditional bulk materials, these nanoscale particles offer the advantage of tailored electronic and optical properties dependent on size due to the quantum confinement effect.[1] The electronic energy levels of a quantum dot become discrete with decreasing particle size, leading to a widening of the energy difference between the valence and conduction bands, also known as the band gap. Consequently, quantum dots exhibit size-dependent absorption and emission spectra. These tunable properties made QDs desirable for a wide range of applications including electronic displays, biological imaging, drug delivery, photodetectors, catalysis, and photovoltaics.[2] To be effectively utilized in these applications, however, QDs in their native hydrophobic form often require surface chemistry modification for improved compatibility.

Current research in QD biocompatibility utilizes multiple methods of stabilizing hydrophobic QDs in polar environments, such as polymer encapsulation, silica coating, direct aqueous synthesis, and ligand exchange. Encapsulation and coating have successfully produced water-soluble QDs, however, these methods increase the hydrodynamic diameter of the particles and require a thick coating, which is inefficient for biosensing applications based on fluorescence resonance energy transfer (FRET).[3] Direct aqueous synthesis, while requiring less processing, yields a broad

QD size distribution with a broad photoluminescent band and occasional defect emission.[4] Published research on the methods of encapsulation, coating, and direct aqueous synthesis consistently report a drop in quantum yield (QY), the standard measurement of quantum dot energy conversion efficiency. The goal of this project is to investigate the method of ligand exchange for the improvement of copper indium disulfide (CIS) quantum dot stability in polar environments. By manipulating the surface chemistry of zinc-sulfide shelled quantum dots, the non-polar, aliphatic thiol ligands can be replaced with -OH capped ligands, improving functionality. This improved hydrophilic functionality and thus, altered QD solubility could unlock future biocompatible applications for high quantum yield, non-heavy metal QDs. Within this thesis, the synthesis of CIS quantum dots followed by a ligand exchange procedure using 11-mercapto-1-undecanol (MUD) recreated from literature[5] and former group experiments will be explored. Characterization of ligand exchange effects on QD chemical composition, optical properties, hydroxy-reactivity, and hydrodynamic radius will then be discussed as a method of better understanding the applications of this method.

EXPERIMENTAL METHODS

SYNTHESIS OF CIS QUANTUM DOTS: Starting reagents for core synthesis were 0.1995 g of copper(I) iodide, 0.4079 g of indium acetate, and 15 mL of 1-dodecanethiol.[6] All reagents were added to a 500 mL three-necked round bottom flask equipped with a magnetic stir bar and thermocouple attached to the reaction heating element. The reaction mixture was degassed under vacuum and purged with nitrogen three times for one hour, thirty minutes, and fifteen minutes, respectively. Under nitrogen atmosphere, the reaction vessel was heated at 220 °C. When an observable

color change from colorless to red was noticed, the reaction was left to heat for 50 minutes and transferred to a cold-water bath. The next day, the shelling procedure was conducted following methods as developed originally by Maya Noesen.[7] Reagents for shelling included 2.6493 g of zinc stearate, 15 mL of avocado oil, and 4.5 mL of 1-dodecanethiol. All reagents were added to the original core product in the round bottom flask and degassed and purged with nitrogen with the same procedure done during core synthesis. The heating mantle containing the round bottom flask was set to 220 °C and the reaction was left to heat for two hours once the measured reaction temperature reached 220 °C.
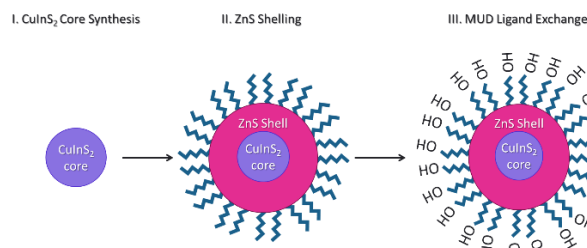

Figure 1. Theoretical depiction of core synthesis, shelling, and ligand exchange steps.

Purification of the synthesis product involved a series of solvent washing, centrifuging, and decanting. A 1:1 mixture of ethanol and methanol were added to test tubes of QD product, mixed sufficiently, and centrifuged for the solvent containing impurities to be decanted. This was repeated with isopropyl alcohol, and again with hexanes – leaving the product in the hexane solution after the final purification step. Removal of solvent via rotary evaporation yielded the final purified native ligand (NL) QDs.

SYNTHESIS OF 11-MERCAPTO-1-UNDECANOL: In a 100 mL round-bottom Schlenk flask equipped with a condenser, 5.024 g of 11-bromo-1-undecanol, 4.56 g of thiourea, and 400 mL of ethanol were combined at room temperature.[8] The solution was then refluxed while stirring at 80 °C for 24 hours under nitrogen atmosphere. The reaction was then cooled to 0 °C via an ice bath. Once at 0 °C, 33.37 mL of ethylenediamine in 100 mL of deionized water was added dropwise via cannula needle, still under nitrogen atmosphere. When all ethylene-diamine solution was added, the reaction was allowed to warm up to room temperature and left to stir under nitrogen atmosphere for 12 hours. The reaction was then decanted into 300 mL of deionized ice water. While at ice water temperature, the mixture was then neutralized using concentrated HCl. The product was then extracted using chloroform and aqueous HCl (25 g HCl in 27.75 mL H2O). The organic layer was isolated via a separatory funnel and eluted through activated aluminum oxide (alumina) via polar column chromatography for further purification. Solvent was removed from the eluate via rotary evaporator and dried under vacuum overnight. The

resulting white solid was stored in the refrigerator until use.
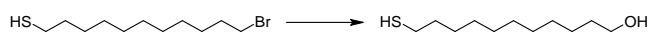
Scheme 1. Starting compound 11-bromo-1-undecanol converted to final product 11-mercapto-undecanol.

Scheme 2. Theoretical depiction of proposed ligand exchange.

11-MERCAPTO-1-UNEDECANOL LIGAND EXCHANGE: The purified native ligand QD product was dried under vacuum overnight to remove any remaining solvent and was washed a second time with a 1:1 mixture of ethanol and methanol and centrifuged to remove remaining impurities. This was repeated a second time with isopropyl alcohol and once again with hexanes, centrifuging a final time to remove any excess unbound ligand. The hexanes solvent was removed via a rotary evaporator and dried under vacuum overnight a second time to yield "double purified" NL QDs.

After the second purification, a 0.3342 g sample of the dried NL QDs was measured out and suspended in 4 mL of 1-octadecene. This solution was then dispersed with a sonicator probe for thirty minutes to break apart aggregates and prevent further clumping before being transferred to a 50 mL round bottom flask equipped with a condenser and a stir bar. Next, 1.8009 g of MUD was added to the reaction flask with any solid MUD stuck to glassware melted into the solution using a heat gun. While in-house synthesized MUD does allow for successful ligand exchange, commercially acquired MUD yields significantly more hydrophilic functionalized product and is preferred.

The vacuum degassing process described during NL QD synthesis was once again performed to maintain an air-free atmosphere. The solution was then heated to 130 °C until reactants were fully mixed, 10-15 minutes under nitrogen atmosphere. Once fully mixed, the reaction was allowed to progress at 210 °C for 15 minutes, still under nitrogen atmosphere.

The ligand exchange QDs were purified in a mixture of ethanol and hexanes, then repeatedly centrifuged to separate polar and non-polar solvent layers. The non-polar hexanes layer was disposed of to remove any remaining DDT and NL QDs. Ethanol solvent was removed from the polar layer containing ligand exchanged QDs via rotary evaporator, with the resulting solid pellet washed a final time with

chloroform to remove excess unbound MUD. The chloroform layer was decanted to leave a solid pellet of QDs. The QDs were last dissolved in ethanol and centrifuged a final time to remove any remaining impurities. The ethanol-dissolved hydroxy functionalized quantum dot product (OH QDs) was then transferred into an air-tight scintillation vial covered in aluminum foil to prevent photo-oxidation, then stored in a refrigerator for future use.

REACTIVITY WITH TOLUENE DIISOCYANATE: Prior to further experimentation, the OH QDs were dried under vacuum overnight to remove any residual solvent or water contamination. With the addition of a hydroxyl group to the QD ligands after the ligand exchange procedure, new solubility behavior was observed, indicating a change in surface chemistry. This change in surface chemistry was further investigated through a toluene diisocyanate (TDI) coupling reaction, wherein the -OH ligand groups would react with added TDI to form new urethane bonds characterizable spectroscopically to determine a successful change in the original molecular structure.

As an experimental control, 1-dodecanol was reacted with TDI to replicate literature results.[9] Under nitrogen atmosphere, 1-dodecanol was dissolved in D6-dimethyl sulfoxide and an equal-molar amount of TDI was added to the solution. This solution was heated to 40 °C while stirring for four hours. This procedure was replicated with OH QDs, with the amount of TDI added being equal-molar to an assumed 100 bonded -OH ligands per QD.

INSTRUMENTATION: Hydrogen nuclear magnetic resonance spectra were obtained via a Bruker Avance III 500 MHz NMR spectrometer. Infrared spectra were obtained with a Thermo iS10 FT-IR spectrometer with ATR accessory. Absorbance spectra were obtained via a Jasco V-670 Ultra-Violet/Visible spectrometer and emission spectra were obtained via a Horiba Fluorolog Fluorometer. QD size characterization was performed via a Malvern Panalytical DLS Zetasizer Advance – Ultra Dynamic Light Scattering (DLS) Particle Size Analyzer.

RESULTS AND DISCUSSION

¹H-NMR AND IR SPECTROSCOPY: In-house synthesized MUD was characterized via ¹H-NMR and IR spectroscopy to assess purification. ¹H-NMR spectra (Fig. 2) of the commercially sourced and in-house synthesized MUD exhibit identical peaks confirming successful synthesis. IR spectra (Fig. 3) demonstrate overlapping key peaks and fingerprint regions. The minor peak present in just the in-house MUD data at 1600 cm⁻¹ was no longer present after alumina filtration, yielding an IR spectrum that nearly perfectly overlapped with the commercial MUD product. Despite these essentially identical spectra, in-house MUD performed poorly when used for QD ligand-exchange compared to the commercially sourced product, suggesting an impurity present not captured by ¹H-NMR and IR spectroscopic

characterization. This impurity is likely a side-product formed via disulfide bonding, which would not be entropically favorable for ligand exchange as compared to the desired thiol. Additional characterization methods, such as mass spectrometry, are needed to confirm the identity of this impurity. Furthermore, a purification method to remove the impurity will need to be developed for in-house synthesized MUD to be a competitive reagent for ligand exchange.
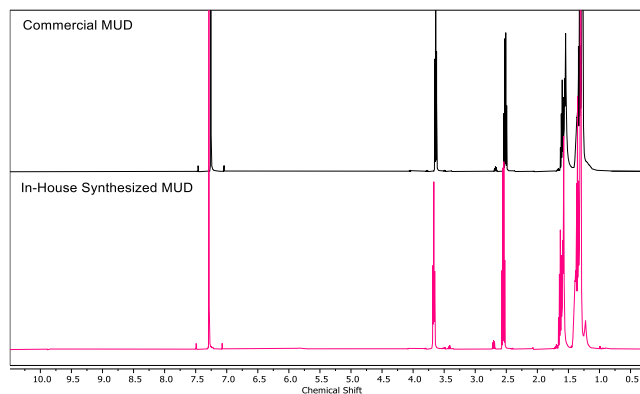

Figure 2. Stacked H¹ NMR spectra of commercially sourced MUD (black) and in-house synthesized MUD (pink) prior to alumina column filtration.
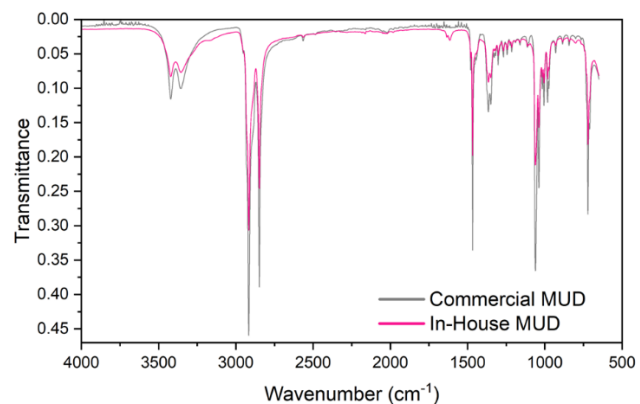

Figure 3. IR spectra of commercially sourced MUD (black) and in-house synthesized MUD (pink) prior to alumina column filtration.

QDs prior to ligand exchange (NL QDs) and after ligand exchange (OH QDs) were characterized via ¹H-NMR spectroscopy. The resulting spectra (Fig. 4) demonstrate modified surface chemistry through hydroxy-functionalization as exhibited in the 3.37 ppm peak present in the OH QD spectra but not present in the NL QD spectra. The appearance of this 3.37 ppm peak post-ligand exchange corresponds to the CH₂OH group of the bound OH ligand, agreeing with previous literature results.
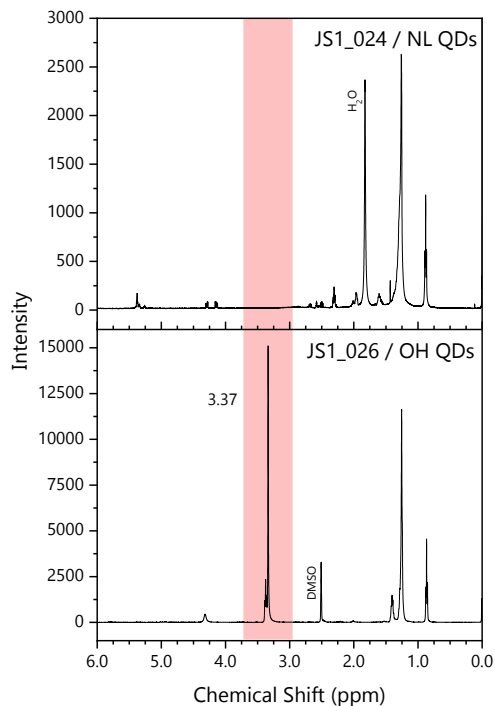
Figure 4. H¹ NMR spectra of NL QDs (top) and OH QDs (bottom) with the appearance of the notable 3.37 ppm CH₂OH peak after ligand exchange highlighted.

These NL QD and OH QD samples were also characterized via IR spectroscopy, yielding the spectra in Fig. 5. Once again comparing with literature results, the broad peak around 3500-3200 cm⁻¹ corresponds to the O-H vibrational stretch of the newly added hydroxy functional group. While the NL QD sample was not dried recently before characterization (as exhibited by the strong water peak in the NMR spectra), the OH QDs were dried under vacuum overnight while heated to 100 °C the day prior to characterization to ensure any hydroxy peaks were not due to contamination.

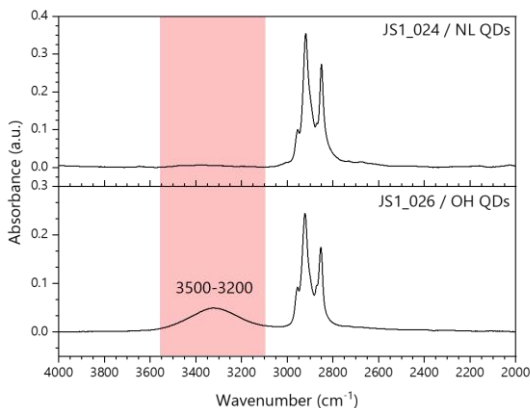**Figure 5.** IR spectra of NL QDs (top) and OH QDs (bottom) with the appearance of the notable 3500-3200 cm⁻¹ O-H vibrational stretch peak after ligand exchange highlighted.

The results of the literature reference agree with the obtained experimental results; however, the literature does not consider the possibility of unreacted, residual MUD which could potentially present with similar spectroscopic peaks. The observed change in solubility behavior of NL QDs being insoluble in ethanol to OH QDs easily dissolving in ethanol implies successful surface modification through the ligand exchange procedure, and thus the resulting experimental spectra is assumed to be in agreement.

ABSORBANCE AND EMISSION: One of the main advantages of ligand exchange as opposed to other methods of surface functionalization is the lack of reduction in emission. While MUD ligand exchange may be successful at improving hydroxy-functionality, if the QY is compromised significantly the method is much less useful for future applications. Thus, the absorbance and emission spectra of the QDs prior to ligand exchange and post-ligand exchange were obtained to compare potential changes in optical properties. As shown in Fig. 6, the absorbance and emission of the NL and OH QDs show no significant differences, indicating the desired optical properties of the quantum dots are retained post-surface modification. The calculated quantum yield of the NL QDs was found to be 67%, while the quantum yield of the OH QDs was found to be 65%. This slight shift in values is suspected to be in part due to error in instrumentation sensitivity and calculation methods, with the QY still remaining relatively high despite ligand exchange.
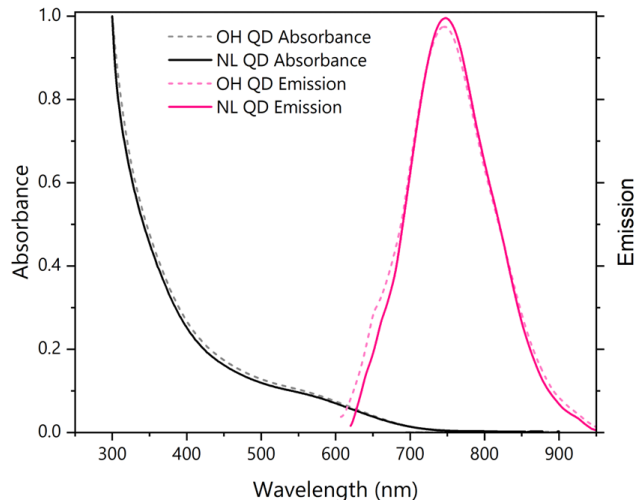

Figure 6. Absorbance (black) and emission (pink) spectra of NL QDs (solid) and OH QDs (dashed).

ANALYSIS OF REACTION WITH TDI: As described in the experimental section, both the control 1-dodecanol and OH QDs were combined with TDI. **¹H-NMR** spectra of 1-dodecanol initially and the product of 1-dodecanol and TDI align with the reference literature results. The included NMR peak identification in the literature for each potential

reaction product acquired by determination of isocyanate group through dibutylamine back titration was used to confirm a successful control reaction and applied to the experimental OH QD results. When comparing the spectra of the 1-dodecanol control product with the OH QD product (Fig. 7), the peaks identified in the literature are present for both indicating successful reaction of the hydroxy functional groups with the TDI. This is evidence that the hydroxy-functionalized ligands are not bound to the QDs too weakly for the further reactions and processing required of biocompatible applications.
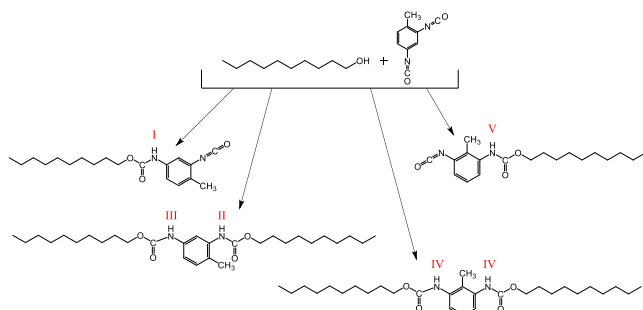
Scheme 4. Potential products of the 1-dodecanol and TDI reaction, as reported in the reference literature.
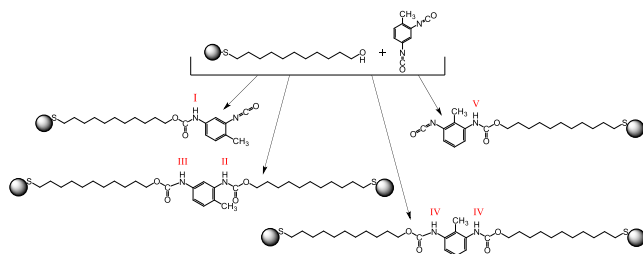
Scheme 5. Proposed potential products of the OH QD hydroxy group reaction with TDI.
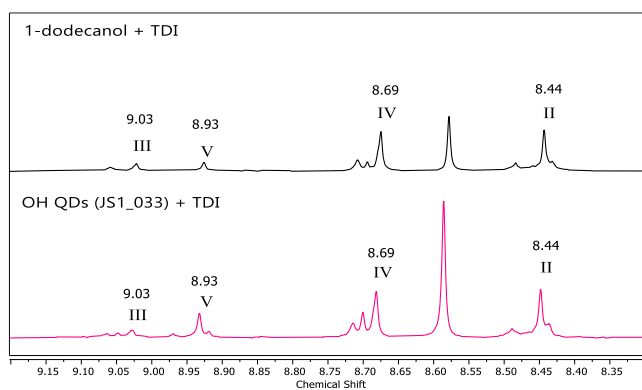

Figure 7. ¹H-NMR spectra of the 1-dodecanol/TDI product (top) and the OH QD/TDI product (bottom). Peaks corresponding to the numeric N-H groups in Schemes 2 and 3 are labeled.

PARTICLE SIZE COMPARISON: Differential light scattering (DLS) was used as a method of qualitative comparison between QD samples. DLS as a characterization of hydrodynamic diameter overestimates true particle size in addition to overstating the relative number of larger-sized particles compared to small particles in polydisperse samples. By comparing the sample volume percent versus diameter, the relative size differences of NL QDs, OH QDs, and OH QDs reacted with TDI. As previously stated, large diameter particles are less efficient in FRET based biosensing, so maintaining the original QD scale as close as possible is ideal. As shown in Figure 8, the NL QDs are represented as the smallest in diameter with a maximum volume percent at 8.30 nm. There is a smaller, broader peak with a maximum volume percent at 17.66 nm, which could be due to any aggregates or large impurities present being overestimated in this sample that was purified only once.

OH QDs after a second purification and ligand exchange, though with a slightly broader dispersion, have a maximum volume percent at 13.06 nm. This small increase in size is still less than that of a polymer encapsulated or a silica coated QDs, which often approach 100 nm in diameter[10] and can encapsulate multiple QDs in a large, aggregated clump. The OH QDs after reaction with TDI appear to be the largest and most polydisperse, with a broad peak across 15 nm to almost 45 nm. The volume percent maximum in this case is 20.53 nm, which is over double the original NL QD size. This is likely due to the intentional coupling of QDs with a urethane linkage as shown in Scheme 5 rather than a reduction in aggregate prevention.

It is also worth noting that these three samples, due to their varying solubility and reactivity, were characterized in different solvent environments. Hydrodynamic diameter may be represented differently in the case of a non-polar molecule in a non-polar solvent as compared to a polar molecule in a polar solvent. Even with this disclaimer, it appears that the hydroxy-functionality and added hydrogen bonding capability of the OH QDs does not significantly increase aggregation of nanoparticles as compared to NL QDs.
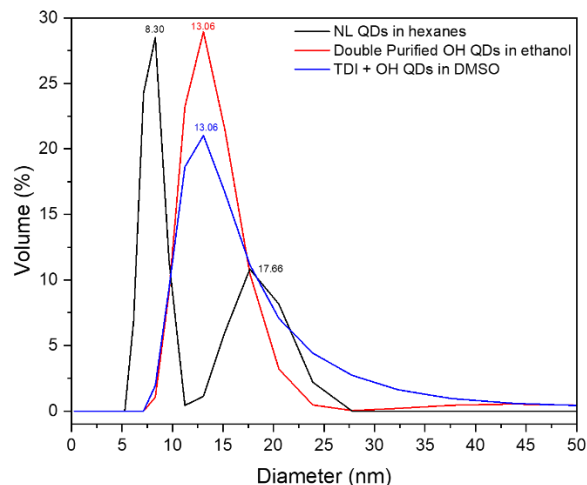
Figure 8. Volume percent versus particle diameter of NL QDs in hexanes, OH QDs in ethanol, and the OH QD/TDI product in DMSO obtained via DLS. The diameters at the maximum volume percentage for each peak are labeled.

CONCLUSIONS

By manipulating surface chemistry through exchanging the native non-polar, aliphatic thiol ligands with hydroxy-capped MUD ligands, the hydrophobic CIS QDs acquire new hydrophilic behavior, making them more suitable for biocompatible or aqueous applications in polar environments. Characterization of the resulting OH QDs confirmed successful surface modification of the QDs through hydroxy-functionalization. ¹H-NMR and IR spectroscopy revealed the presence of hydroxy functional groups bound to the OH QDs after the ligand exchange, validating this method. The absorbance and emission spectra of the QDs before and after the ligand exchange showed no significant differences, indicating that the desired optical properties of the QDs were retained post-surface modification. The quantum yield of the QDs remained relatively high with little change, suggesting that this method of ligand exchange did not compromise their energy conversion efficiency.

Furthermore, the reactivity of the hydroxy-functionalized QDs with toluene diisocyanate (TDI) was examined as a proof of concept for further reactions post-ligand exchange. The H¹ NMR spectra confirmed the successful reaction of the hydroxy groups with TDI, forming urethane bonds mirroring that of the literature and experimental control results with 1-dodecanol. This demonstrated that the hydroxy-functionalized ligands are sufficiently bound to the QDs for the further reactions and processing required for use in future applications.

Particle size comparison through DLS revealed that the ligand exchange process and newly acquired hydrogen bonding abilities slightly increased the QD diameter but still maintained it within an acceptable range for applications

such as biosensing. This size increase is still relatively smaller when compared to other functionalization methods such as polymer encapsulation or silica coating.

Overall, the method exchanging native ligands with MUD has been shown to effectively enhance the stability and functionality of CIS quantum dots. The results demonstrated the feasibility of using ligand exchange to modify the surface chemistry of QDs, enabling their potential application in various fields such as electronic displays, biological imaging, drug delivery, photodetectors, catalysis, and photovoltaics. Additional investigation into quantifying the ligand exchange yield, as well as how environmental factors like pH affect the stability of these OH QDs is still needed. Further studies can focus on optimizing this ligand exchange process and exploring the potential for specific applications of these hydrophilic, high quantum yield CIS QDs in different domains of nanotechnology.

AUTHOR INFORMATION

Corresponding Author

* Julia Schexnayder, schexnj@wwu.edu

REFERENCES

References

1. Chakraborty, T. *Quantum Dots: A Survey of the Properties of Artificial Atoms*, 1st ed.; Elsevier Science B.V., 1999.

2. Cotta, M. A. Quantum Dots and Their Applications: What Lies Ahead? *ACS Applied Nano Materials* **2020**, *3* (6), 4920–4924. DOI:10.1021/acsanm.0c01386.

3. Medintz, I. L.; Konnert, J. H.; Clapp, A. R.; Stanish, I.; Twigg, M. E.; Mattoussi, H.; Mauro, J. M.; Deschamps, J. R. A Fluorescence Resonance Energy Transfer-Derived Structure of a Quantum Dot-Protein Bioconjugate Nanoassembly. *Proceedings of the National Academy of Sciences* **2004**, *101* (26), 9612–9617. DOI:10.1073/pnas.0403343101.

4. Hildebrandt, N.; Spillmann, C. M.; Algar, W. R.; Pons, T.; Stewart, M. H.; Oh, E.; Susumu, K.; Díaz, S. A.; Delehanty, J. B.; Medintz, I. L. Energy Transfer with Semiconductor Quantum Dot Bioconjugates: A Versatile Platform for Biosensing, Energy Harvesting, and Other Developing Applications. *Chemical Reviews* **2016**, *117* (2), 536–711. DOI: 10.1021/acs.chemrev.6b00030.

5. Kim, H.; Suh, M.; Kwon, B.-H.; Jang, D. S.; Kim, S. W.; Jeon, D. Y. In Situ Ligand Exchange of Thiol-Capped CuInS2/ZnS Quantum Dots at Growth Stage without Affecting Luminescent Characteristics. *Journal of Colloid and Interface Science* **2011**, *363* (2), 703–706. DOI: 10.1016/j.jcis.2011.06.087.

6. Li, L.; Pandey, A.; Werder, D. J.; Khanal, B. P.; Pietryga, J. M.; Klimov, V. I. Efficient Synthesis of Highly Luminescent Copper Indium Sulfide-Based Core/Shell Nanocrystals with Surprisingly Long-Lived Emission. *Journal of the American Chemical Society* **2011**, *133* (5), 1176–1179. DOI:10.1021/ja108261h.

7. Noesen, M. Robust and Simple Synthesis of CIS/ZnS Refined for High Luminescence in the Near-IR. WWU Honors Program Senior Projects, Western Washington University, Bellingham, WA, 2020. https://cedar.wwu.edu/wwu_honors/402

8. Tanaka, M.; Sawaguchi, T.; Sato, Y.; Yoshioka, K.; Niwa, O. Synthesis of Phosphorylcholine–Oligoethylene Glycol–Alkane Thiols and Their Suppressive Effect on Non-Specific Adsorption of Proteins. *Tetrahedron Letters* **2009**, *50* (28), 4092–4095. DOI:10.1016/j.tetlet.2009.04.091.

9. Hu, Q.; Huang, G.; Zheng, J.; Su, H.; Guo, C. Synthesis and Rheological Properties of Hydrophobically Modified Poly(Vinyl Alcohol). *Journal of Polymer Research* **2012**, *19* (12). DOI:10.1007/s10965-012-0006-3.

10. Yang, Y.; Jing, L.; Yu, X.; Yan, D.; Gao, M. Coating Aqueous Quantum Dots with Silica via Reverse Microemulsion Method: Toward Size-Controllable and Robust Fluorescent Nanoparticles. *Chemistry of Materials* **2007**, 19 (17), 4123–4128. DOI:10.1021/cm070798m.